Supplemental Materials

Molecular Biology of the Cell

Sellou et al.

The poly(ADP-ribose)-dependent chromatin remodeler Alc1 induces local chromatin relaxation upon DNA damage

Hafida Sellou, Théo Lebeaupin, Catherine Chapuis, Rebecca Smith, Anna Hegele, Hari R. Singh, Marek Kozlowski, Sebastian Bultmann, Andreas G. Ladurner, Gyula Timinszky, and Sébastien Huet

SUPPLEMENTAL INFORMATION

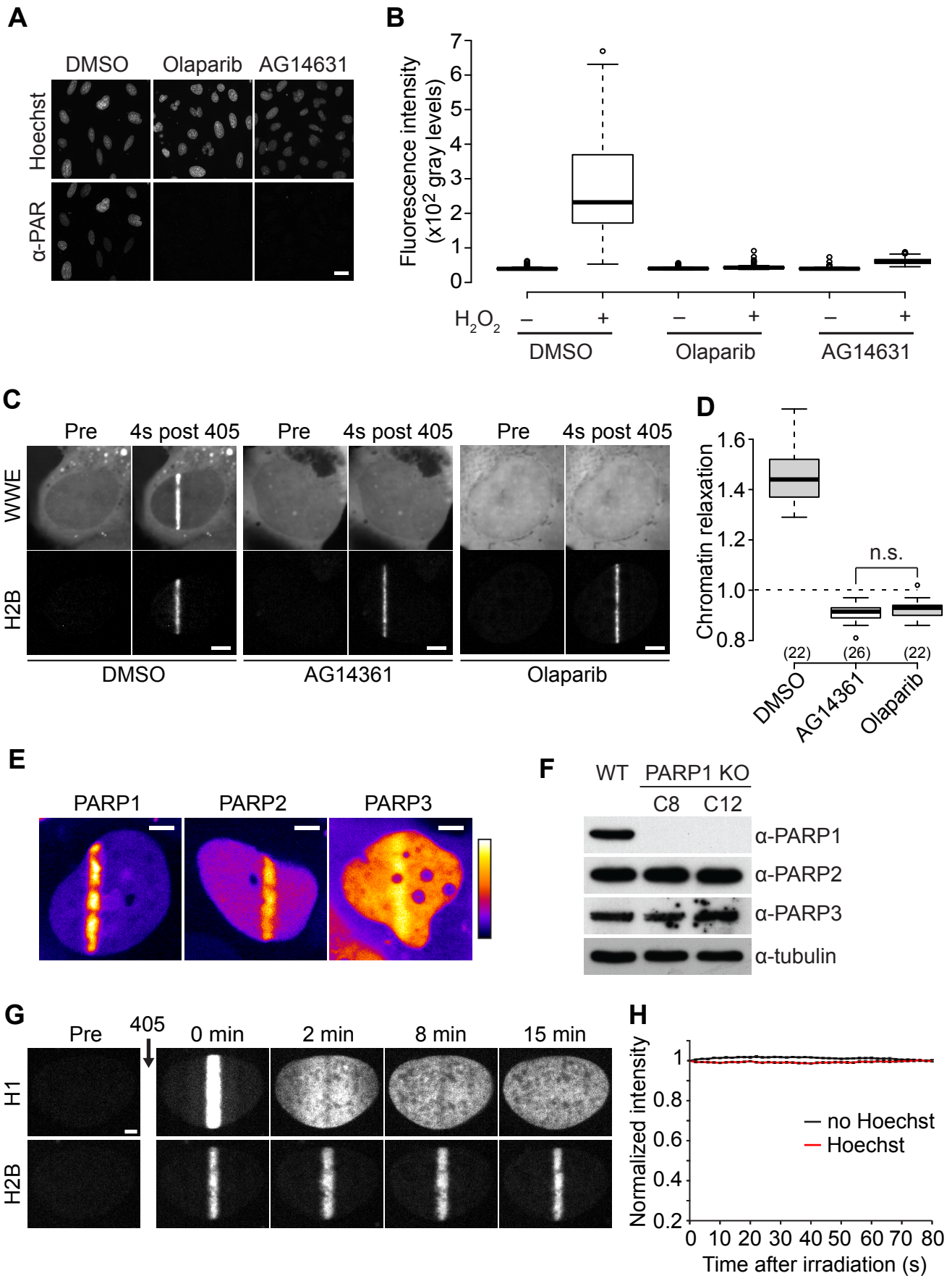

Sellou et al., Figure S1

Figure S1: PARP1-dependent chromatin dynamics at DNA damage sites. (A) Confocal images of immunofluorescence staining with anti-PAR (10H) antibody performed in U2OS cells treated or not with PARP inhibitors. The PARP1 inhibitors AG14361 and Olaparib were used at 30 μM and 50 μM, respectively for 1 hour before H_2O_2 treatment. DNA damage was induced by treating the cells with 0.5 mM H_2O_2 in PBS for 10 min. Bar = 25 μm. For the fluorescence quantification (B), nuclei were segmented using Hoechst staining and the mean fluorescence intensity for the anti-PAR antibody was measured inside each nucleus. (C) Recruitment at DNA damage sites of the PAR-binder WWE domain of RNF146 in cells co-expressing WWE-EGFP and H2B-PATagRFP, pre-sensitized with Hoechst and treated or not with the PARP inhibitors AG14361 (30 μM, 1h) or Olaparib (50 μM, 1h). Bar = 4 μm. The strong recruitment of the WWE domain observed at DNA lesions in the control cells was completely abolished upon treatment with AG14361 or Olaparib, demonstrating the efficiency of these inhibitors. (D) Relative chromatin relaxation at 60s after laser micro-irradiation in U2OS cells expressing H2B-PAGFP and treated or not with the PARP inhibitors AG14361 (30 μM, 1h) or Olaparib (50 μM, 1h). (E) Recruitment of human PARP1, PARP2 and PARP3 at DNA damage sites induced by laser micro-irradiation. U2OS cells were transfected with GFP-tagged PARP proteins. Images were taken 2 minutes after laser irradiation. Bar = 4 μm. Fluorescence signals are pseudocolored using the lookup table shown on the right of the images. (F) Western-blot of wild type U2OS cells and the two knockout cell lines showing the relative amount of PARP1, PARP2 and PARP3 in the different cell lines. (G) Confocal image sequence acquired at long time scales for a U2OS cell co-expressing H2B-PATagRFP and H1-PAGFP. For the H1 channel, the image contrast was enhanced to allow the visualization of H1 redistribution over the entire nucleus following laser micro-irradiation. This led to an apparent saturation of the image at time = 0s. Bar = 4 μm. (H) Kinetics of H2B release from the irradiated line in wild-type U2OS cells expressing H2B-PATagRFP and pre-sensitized (n=18) or not (n=20) with Hoechst (mean ± SEM).

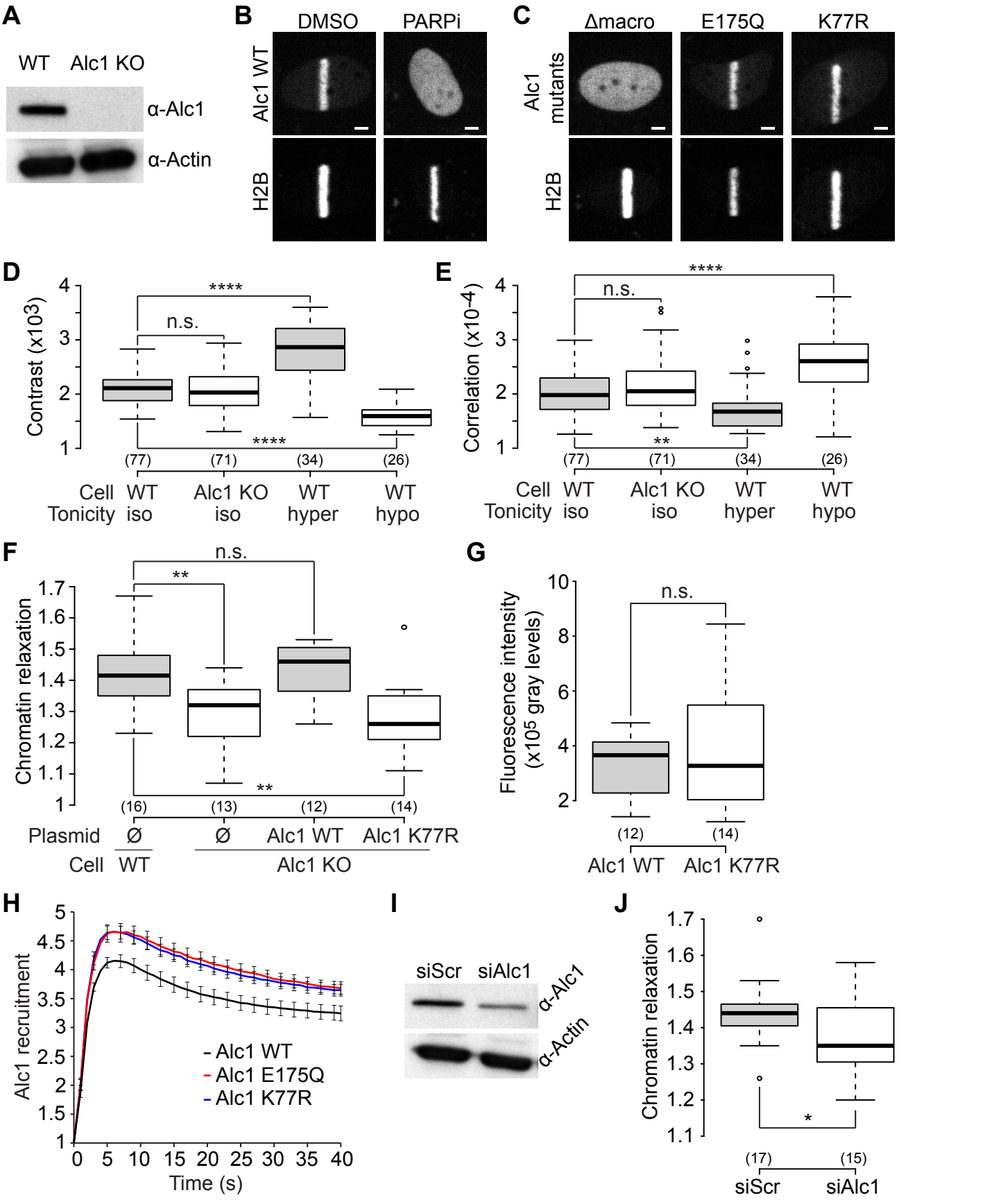

Sellou et al., Figure S2

Figure S2. The chromatin remodeler Alc1 is involved in chromatin relaxation at DNA damage sites. (A) Western-blot of wild type U2OS cells and the Alc1 knockout cell line. (B) Recruitment of Alc1 at the DNA damage sites in cells co-expressing the wild-type version of Alc1 fused to mCherry and H2B-PAGFP. Cells were pre-sensitized with Hoechst and treated or not with the PARP inhibitor AG14361 (30 μM, 1h). Images were acquired 10 s after laser micro-irradiation. Bar = 4 μm. The recruitment of Alc1 at DNA lesions was fully abolished upon treatment with AG14361. (C) Recruitment of Alc1 mutants at the DNA damage sites in cells co-expressing Alc1 mutants fused to GFP or YFP and H2B-PATagRFP. The Alc1-Δmacro is lacking the macro domain and the Alc1-E175Q and Alc1-K77R are two ATPase-dead mutants. Cells were pre-sensitized with Hoechst. Images were acquired 10 s after laser micro-irradiation Bar = 4 μm. The recruitment of Alc1 at DNA lesions was fully abolished for the Alc1 mutant lacking the macro domain but not for the ATPase-dead mutants. (D-E) Quantitative analysis of the Hoechst patterns in wild-type and Alc knockout U2OS cells. Two parameters were assessed to characterize the chromatin compaction state: the contrast (D) and the pixel-to-pixel correlation (E). As positive controls, we analyzed the chromatin patterns in cells bathed with hypertonic or hypotonic medium to induce chromatin hyper-compaction or decompaction, respectively. (F) Relative chromatin relaxation at 60s after laser micro-irradiation for wild type cells versus Alc1 knockout cells co-transfected with H2B-PAGFP and an empty plasmid (Ø), wild-type Alc1 or the catalytic-dead mutant Alc1 K77R, both fused to mCherry. (G) Integrated fluorescence signals in the mCherry channel measured for the nuclei studied in (F) and expressing the wild-type and K77R Alc1 constructs fused to mCherry. (H) Kinetics of Alc1 recruitment at the DNA lesions measured in Alc1 knockout cells co-expressing H2B-PATagRFP and different Alc1 constructs fused to GFP. Three Alc1 constructs were analyzed: a wild-type version and two ATP-ase dead mutants E175Q and K77R (mean ± SEM, $26<n<34$). (I) Western-blot of U2OS cells treated with a scrambled siRNA or with a siRNA directed against Alc1. (J) Relative chromatin relaxation at 60s after laser micro-irradiation for wild type U2OS cells stably expressing H2B-PATagRFP and transfected with a scrambled siRNA or a siRNA directed against Alc1.